

# Adsorption Characteristics of Ekowe Clay and Uptake Kinetics of Methylene Blue onto the Raw and Modified Clay

Daniel C. Emeniru<sup>1</sup>, Okechukwu D. Onukwuli<sup>2</sup>, Pere-ere Douye Wodu<sup>3</sup> and A. O Momohjimo<sup>3</sup>

<sup>1</sup>Department of Petroleum Engineering and Geo-Science Technology, Federal Polytechnic, Ekowe, Bayelsa state, Nigeria

<sup>2</sup>Department of Chemical Engineering, NnamdiAzikiwe University, Awka, Anambra state, Nigeria

<sup>3</sup>Department of Science Laboratory Technology, Federal Polytechnic, Ekowe, Bayelsa state, Nigeria

**Abstract**– The uptake capacity and MB affinity of clay adsorbent is largely dependent on the mineral composition as well as site orientation and availability of the clay adsorbent. The characteristic of Ekowe clay as revealed in the pH, PZC, CEC, FTIR, and the porosity and enhanced surface area influenced by the modifications showed morphological and structural changes that resulted in the high adsorption potential of the clay. The modification improved total surface area portrayed RS-22.04m<sup>2</sup>g<sup>-1</sup>, RCS-30.36m<sup>2</sup>g<sup>-1</sup> and ACS-40.92m<sup>2</sup>g<sup>-1</sup>. Mineralogy (FTIR) revealed the presence of admixtures. PZCs < solution pH indicated cation affinity, capability of floc formation and enhanced dye adsorption. Statistical regression, error analysis as well as  $q_{e,exp}$  and  $q_{e,cal}$  agreement showed the Lagergren pseudo-second-order kinetic model as best fit to the experimental data. Intra-particle diffusion and diffusion resistance gave contributive control to the rate at which the MB diffused to and from the clay surfaces.

**Keywords**– Adsorption, Activation, Calcination, PZC, CEC, FTIR and Kinetics

## I. INTRODUCTION

Since we cannot make or produce water it is necessary to manage and conserve the much nature has made available.

As a major component of agriculture and manufacturing, good water management is very essential for good health and comfort, the end purpose to every human endeavour. Up to 70% of the world's water usage is involved in food production, both natural and industrial.

The ground serves as water reservoir where surface waters drain-into forming underground water, the major source of drinking water for more than one-half of the world's population, both the rural and urban communities. Population explosion, haphazard rapid urbanization, industrial and technological expansion, energy utilization and waste generation from domestic and industrial sources have rendered the soil and its surface and underground waters unwholesome and hazardous to man, living organisms and the environment around them.

Problems in domestic and industrial water quality include presence of inorganics (elements and compounds), organic matters, and variety of pathogens. These contaminants are the

major causes of various water-borne diseases, food poisoning, and the breakdown of some industrial machinery.

There are little or no stringent laws guiding environmental pollution in many nations: Yasin et al., 2007; Chatterjee et al., 2009; Rahman, et al. 2012; Gulnaz, et al. 2004 and Velmurugan et al., 2011 have reported recent global anthropogenic activities are solely responsible for the introduction of dye into water bodies. In spite the preventive measures in textile and colour allied industries; coloured effluent arises as a direct result of production of the dye, its use and the use of finished products of dye composition.

Dye in wastewater is highly visible and can obstruct light penetration which is highly threatening to aquatic lives (Chang, et al. 2004). Spontaneous photo and thermal remediation measures of dye removal in liquid effluents are non-viable as a result of its high stability to heat and light irradiation. Nasra et al., (2006) have reported dyes to be responsible for low biochemical oxygen demand (BOD) and high chemical oxygen demand (COD). Dye has been cited to be dangerous, mutagenic and carcinogenic in nature (Crini, 2006 and Safa & Bhatti, 2011), can destroy or inhibit metabolism in some microorganisms, has defied biodegradation, and its removal from wastewater has been very stringent due to its complex structure and synthetic origins.

Methylene blue is a basic dye that has gained extensive uses in different fields; biology, chemistry, medicine (microbiology, surgeries, diagnostics) (Rahman et al., 2012) and also in textile industries. It is not significantly metabolized by the liver if ingested; resists stomach acidity; and can quickly be filtered out by the kidneys. Methylene blue has been used particularly for adsorption studies, not only because of its environmental concern but also for the fact that it has been recognized as a model adsorbate for the removal of organics (Hameed et. al., as cited in Abechi, et al. 2011). It has been used extensive to study adsorption onto low cost adsorbents: Rice Husk (Safa & Bhatti, 2011, Rahman et al, 2012), palm kernel shell (Abechi, et. al., 2011), and Coconut shell (Yasin et. Al., 2007).

Adsorption over the years has remained a successful technological procedure for colour removal from effluents using natural and modified adsorbents. Adsorption is a

process by which atoms, molecules or ions are retained on the surfaces of solids by chemical or physical bonding. The degree of adsorption of any specie (adsorbent or adsorbate) is primarily dependent on the inherent characteristics of the adsorbent specie: hydrogen potential (pH), Point of Zero Charge (PZC), Cation Exchange Capacity (CEC), and the mineral composition and structure; a Fourier Transform Infra-Red (FTIR) determinate. During adsorption, adsorbates first diffuse from bulk to external surface of the adsorbent then migrates (transport process-Fick's law) from adsorbent external surface via pores into the internal surface where the molecules adhere onto the surfaces (adsorption sites). This well describes the adsorption kinetics, a major requisite and aspect of adsorption studies and system design.

The Kinetic models are typical with fundamental description of the interactive behavior between adsorbate and adsorbent. The choice of a model is its applicability over the entire range of process conditions. Bearing in mind that models are mainly mechanisms, the model of best fit would show best curves and graphs representing the model equation that elucidate the adsorption system. Note: Model fitness does not imply the model represents what actually happens in the system under study, also difference in fit can be explained entirely in terms of experimental errors which statistically the difference may not be significant. Therefore, it is reasonable that the simplest and easiest-to handle equations of satisfactory fit be considered in a study. It is factual to choose the less complicated of two models that equally fit a data. Notwithstanding, finding the correct model has shown some difficulty even in the most carefully conducted programme of experimentation; owing that the magnitude of the experimental error will very likely mask the differences predicted by the various mechanism. It is therefore hardly ever possible to determine with reasonable confidence which is the correct model. In adsorption study; kinetics, against all odds, analysis has basically been on Lagergren Pseudo first and second order, Elovich, Intra-particle diffusion, and pore diffusion resistance.

Characteristic advantages have been recorded with the use of low cost adsorbents: efficiency, low investment and operational cost, minimum chemical sludge formation and possible regeneration. Though many adsorbents such as activated carbon, peat, chitin, and others have proved quite effective in colour removal, there are flaws of concerns in affordability, availability, application friendliness, etc which has been taken care of with the advent and application of clay. Studies have proven clay adsorbent recyclable (regeneration), abundant (availability), cheap (affordability) and user/application friendly. Clay adsorbent compared with activated carbon and other adsorbents has shown equivalent and in some studies better potency in dye removal from aqueous solutions.

Clays are extremely fine particles exhibiting chemical properties of colloids (Wikipedia: Deer, W. A. 1985). Clay minerals are fine hydrous aluminum silicates with large interlayer space that can hold significant amounts of water and other substances and are encompassed of large surface area that allow swelling and shrinking. Clay minerals typical with the adsorptive removal of water contaminants have been categorized with 1:1 and 2:1 phyllosilicates been most

popular and comprising the following groups: Smectite, Kaolinite, Illite, chlorite, etc. Clay types like Montmorillonite, Kaolinite, Bentonit, and Illite are widely preferred and used because of their high specific surface area, chemical and mechanical stability, a variety of surface and structural properties, abundance and low cost (Bailey, et. al., 1999).

The findings of this study would encourage the use of abundant local clays as competitive alternatives, reduce the risk of local carbon activation, and reduce the use of high sludge generating methods. Numerous abundant locally sourced clays of competitive and substitutive viability to activated carbon have not been considered for study. Though clay and its modified forms have been reported as good adsorbent for dye removal from aqueous solution, the adsorption propensity of Ekowe clay, raw and modified, has not been verified. Ekowe clay is a clay obtained from a hamlet, Ekowe, in Southern Ijaw LGA, Bayelsa state Nigeria. Activation of clay is very common in the literatures however; calcination has not gained wide application as a viable modification technique. Besides the work of Talaat et. al., (2011) which reported very poor Heavy Metal uptake unto activated calcined Kaolinite, no study has considered the effect of calcination on raw and activated Ekowe clay for Methylene Blue uptake.

This study seeks to apply activation and calcination in an attempt to modify a Nigerian clay into a valuable clay adsorbent for dye removal from aqueous solution and as well strengthen, expand and validate the findings of related studies.

## II. MATERIALS AND METHOD

### A) Materials

The equipment, apparatus and all the chemicals; analytical grade reagents, solid granules and powders, used were properties of Springboard Laboratory, Udoka Housing Estate, Awka, Anambra state.

### B) Adsorbent Preparation

The crude clay, mined from an excavated swampy site at Federal Polytechnic Ekowe, Bayelsa state was first purified by washing in its source water to remove sand and suspended organic matter. Then washed trice with distilled water to remove impurities (dissolved chemicals impurity) relative to the source water. The purified raw clay was allowed to dry at ambient temperature for four (4) days, covered with sieve cloth material to prevent dust and other solid impurities. The purified clay was further dried in an oven at 45°C for about 24hrs and referred as raw clay, RS. The raw Ekowe clay sample (RS) was modified by activation and calcination to suit the requisite samples scoped for this study.

A quantity of RS was mixed with sufficient amount of 0.5M H<sub>2</sub>SO<sub>4(aq)</sub> solution in a beaker and mixture was heated in an electronic thermostatic water tank for 3hrs at 90°C. The heated mixture was allowed to cool, decanted and the activated clay sludge was washed with distilled water until it was free of SO<sub>4</sub><sup>-2</sup> ions by indicating a neutral pH (≈7) with a pH indicator paper. The activated sample was dried in an oven at 40°C for 3hrs and crushed. Raw and activated samples were calcined in a muffle furnace at 750°C for 4hrs to produce raw-

calcined sample (RCS) and activated-calcined sample (ACS). The calcined samples were cooled in a desiccator, crushed and sieved with 75 $\mu$ m sieve (200 Mesh ASTM). The RS, RCS and ACS were packaged in polyethylene bags and stored to be used for the adsorption experiment.

### C) Solution Preparation

All solutions' (stock and experimental concentration) preparation applied the dilution theory using predetermined quantities of solid/granule/liquid chemicals and distilled water.

5g commercial Methylene Blue (MB) (C<sub>16</sub>H<sub>18</sub>N<sub>3</sub>SCl.3H<sub>2</sub>O) was dissolved in distilled water to produce 5g/L dye stock solution. The experimental concentrations (20, 25, 30, and 35mg/L) were obtained by dilution.

### D) Characterization

**pH:** Soils with more clay or organic matter have a greater ability to resist pH changes (Bob Lippert). Clay and organic matter in the soil tends to store acidity. Active acidity of clay/soil preparation can be measured with litmus paper, indicator solutions or a pH electrode. 1g of each sample (RS, RCS, ACS) was added to 10ml of distilled water, stirred vigorously and the pH of the suspension was then measured using the pH meter.

**Acidity of Raw clay:** The work of Touillaux et al. (1967) has revealed that dissociation of water molecule adsorbed on clay surface is far greater than in liquid water. This affirmed that the hydration water of clay minerals is most often acidic. Acidity of clay minerals is strongly affected by the exchangeable cations and the degree of hydration of the clay. The greater the polarizing ability of the interlayer cations, the stronger and more numerous the acid sites (Frenkel, 1974). It is also affected by the position of the negative charge where it is noticed that isomorphic substitution on the octahedral sheet seems to cause stronger acidity than corresponding acidity of the tetrahedral sheet (Frenkel, 1974). Estimation of acidity of clay mineral using colour change of phenolphthalein indicator has been reported.

5g of clay was boiled for 3min. with 10ml distilled water then filtered and washed with another 50mL of distilled water. The filtrate was titrated with 0.1N NaOH<sub>(aq)</sub> to phenolphthalein end point. The acidity (% wtNaOH/g clay).

$$\text{Acidity} = [(V \times N \times 40) / W_c] \times 100 \quad (1)$$

Where V is the titre volume of NaOH<sub>(aq)</sub>(ml), N is normality of NaOH<sub>(aq)</sub> and W<sub>c</sub> is weight of clay (g).

**Cation Exchange Capacity:** The CEC was determined by the Potassium chloride leaching method. Ideally, clay soils with considerable CEC will range realistically in the 1-5% potassium, 10-15% magnesium, 65-75% calcium and sodium <1%. In CEC evaluation, exchangeable acidity is added to the sum of extractable Ca<sup>2+</sup>, Mg<sup>2+</sup> and K<sup>+</sup>, for soils (clay) of pH < 6, reflecting that significant quantities of exchangeable Al<sup>3+</sup> may be present. Sodium is neglected due to low percentage composition, and in some case, like in this

work, the percentage composition of K was neglected as KCl was used as the leaching agent.

**Procedure:** 25ml of 1MKCl<sub>(aq)</sub> was mixed with 5g dry RS in an Erlenmeyer flask and stirred thoroughly using the magnetic stirrer. The mixture was filtered using filter paper; filtration was repeated three times by adding 25ml 1MKCl<sub>(aq)</sub> on the clay residual and allowed to drain completely before adding the next. 1ml Sr(NO<sub>3</sub>)<sub>2</sub> (strontium Nitrate) was added into 25ml of each leachate in an Erlenmeyer flask. The exchangeable Ca and Mg in the filtrates were evaluated in ppm using the Atomic Adsorption Spectrophotometry (AAS). This procedure was repeated for RCS and ACS.

For the exchangeable acidity, 5 drops of phenolphthalein indicator was added into 25ml of each filtrate in a Erlenmeyer flask. On a magnetic stirrer, 0.01M NaOH<sub>(aq)</sub> was titrated against the filtrate until a faint pink colour appeared. The exchangeable acidity is given as a product of titre value and Correction factor, CF of 8.

$$\text{CEC}_e = \text{Exchangeable Ca} + \text{Exchangeable Mg} + \text{Exchangeable acidity (H)} \quad (2)$$

**Filtration Rate:** Filtration rate depicts clay sample's capillarity, water retention capacity and interaction tendency with adsorbate. The shorter the time of filtration the higher the rate: apparently, implying high porosity of the sample relative to the surface area. The filtration rate of the clay sample was determined using suction filtration method. 1g of each sample was mixed with 15ml of distilled water and filtered using Filter paper. After the initial water had been filtered from the sample, a further 50 ml was poured in glass tap burette and the water added at a regulated rate such that the volume in the filter paper is constant till the content of the burette is discharged. The filtration time was recorded for the 50mL distilled water. The filtration rate was determined according to the method adopted by Bahzal, et al. (1975) and Khraisheh, et al. (2004) for diatomite:

$$V_F = \frac{W_F}{vt} \quad (3)$$

Where V<sub>F</sub> is the filtration rate (ml/m<sup>2</sup>s<sup>1</sup>); W<sub>F</sub> the volume of the filtrate (ml); F the effective filter paper surface (m<sup>2</sup>), and t is the filtration time (s).

**Point of Zero Charge (PZC):** Considering the salt addition method of PZC determination, 0.4g of RS was added into six Erlenmeyer flasks containing 20mL 0.1M KNO<sub>3(aq)</sub>. Same was done for RCS and ACS. Initial pH values of the six solutions for each sample were adjusted to 3, 4, 6, 7, 9 and 11 by adding few drops 0.1M HNO<sub>3(aq)</sub>. The mixtures were allowed to equilibrate at 25°C in isothermal shaker for 24hrs and filtered. The pHs of the filtrates were measured as final pHs. The PZC was estimated from a plot of  $\Delta$ pH vs pH<sub>0</sub>. The value at the point that cuts pH = 0 line of the  $\Delta$ pH vs pH<sub>0</sub> plot gives the PZC for each sample. The average PZC for two trials was used for each sample (Arlette et. al., 2012).

**Surface Area:** This work adopted Sears' method as proposed by G. Sears, (1956) for the surface area determination of the clay samples. The method has gained

wide application in clay studies; Al-Degs, et al. (2001); Shawabkeh and Tununji, (2003); Khraisheh et al., (2004); Bhattacharyya and Gupta (2006) & (2009); Osmanlioglu, (2007).

Applying same procedure for RS, RCS and ACS; 0.2g of sample was mixed with 15mL of distilled water in a flask and acidified with dilute acid (HCl) to pH4. 5g NaCl<sub>(s)</sub> was added and the volume made up to 25mL with distilled water. The solution was titrated with 0.10M NaOH<sub>(aq)</sub> observing the pH. The volume (V) required to increase the pH from 4 to 9 was recorded. The volumetric analysis was duplicated for each sample and the average used for surface area calculation (ALzaydien, 2009). The surface area (S) according to Sear's method was estimated as:

$$S \text{ (m}^2\text{g}^{-1}\text{)} = 32V - 25 \quad (4)$$

#### **Fourier Transform Infra-Red (FTIR) Spectroscopy:**

Alkali-halide disks (e.g., KBr) formed from oil mulls (e.g Nujol-paraffin oil), one of the various sample preparation techniques for FTIR (Transmission spectroscopy), was used in the FTIR spectra production. Being dried samples, popular 15min preheating was ignored therefore samples were analyzed directly without any heating.

1g of powdered sample was crushed with 0.5gKBr using the BUCK 530 IR mortar. 1ml of the Nujol paraffin oil was added into the sample to form a paste. The paste was introduced into the sample mould of the IR spectrophotometer and scanned at a wavelength of 600 – 4000nm to produce the spectra lines.

#### **E) Batch adsorption studies**

Batch process has been mostly used in experiments where concentration and rate are of the essence. Being that the influence of adsorption factors such as pH, contact time, initial concentration, adsorbent concentration/amount, temperature are to be considered, batch mode has been ascertained and frequently used as the best mode that will provide runs on which the factor effects can be checked. Duplication of experimental runs is known to authenticate and ascertain regularity of experimental values for parameters determination. The mass balance equation below gives the adsorbate uptake onto the adsorbent:

$$q_t = \frac{C_0 - C_t}{m} V \quad (5)$$

$q_t$  is the dye uptake after the experimental time (g/g),  $C_0$  and  $C_t$  are the dye concentrations at  $t=0$  and  $t=t$ , m is the amount of clay used and V is the volume of dye solution.

**Experiment:** Blank runs (without clay) were undertaken using 50mL MB solutions of 25mg/L and 35mg/L at the solution pH 7.20 and 40°C for 50min. The solution was handled as though in an actual run with adsorbent so as to verify if the glass wall partakes in the dye adsorption. Though flask walls showed no adsorption of the dye solution, it was noticed, the dye stains the walls of glassware after 24hrs of stocking the solution. Therefore, dye solutions were prepared and used daily.

In the kinetics study, time and dye concentration were varied (20, 50, 80, 110, 140, and 170Min.; and 15, 20, 25, 30 and 35mg/L) at constant solution volume (0.03L), pH (5.5), Clay amount (0.3g), and Temperature (27°C). The use of centrifuge was employed after each time interval to obtain the residual solution and the residual dye concentration was determined from the Absorbance obtained using the APEL PD-3000UV spectrophotometer at a wavelength of 610nm. The spectrophotometer absorbances were converted to concentrations using linear calibration graph.

### III. RESULTS AND DISCUSSION

#### **A) Characterization**

**pH and Point of Zero Charge:** The pH of the samples as reported in Table 1 showed acidic samples. It is known that silica containing materials precipitate (dissolve) when exposed to alkaline solution (Khraisheh, et al. 2004) therefore the clay samples are stable in their acidic states. Sorbents exhibit amphoteric nature depending on PZC/pH relationship; being anion exchanger at PZC>pH and cation exchanger at PZC<pH of suspending solution. For sorbent pH above it's PZC, the surface displays cation exchange ability and vice versa for anion at sorbent pH<PZC (Appel et al., 2003). This implies the clay has a high Mb dye adsorption potency.

PZC, the negative logarithm of the *activity* of the potential-determining ion in the bulk fluid, is solely pH dependent factor depicting the pH at which colloidal particles, if submerged in an aqueous ionic solution, exhibits zero net electrical charge on the surface. In order to maintain electro-neutrality, polyvalent counter-ions in aluminosilicates reverse the zeta(ζ)-potential of the clay surface owing to distance between surface charges ( $7^{-10}$  Å) (Tschapek, et al. 1974). Nonexistence of pure clay mineral and electrophoretic mobility studies have revealed there is no factual PZC for any known clay mineral. Heating above 200°C increased the PZC of a clay mineral (Tschapek, et al. 1974), however the PZCs as shown in Table 1 reported decreased PZC for RCS and ACS; probably due to thermal formation of low PZC admixtures, increased SiO<sub>2</sub> due to thermal dissociation of Si-O-(Al/Fe), and thermal dehydroxylation. In accordance with the pH-PZC principle of cation attraction at solution pH > clay PZC the samples' PZC as shown in Table 1 indicate their capacity for MB dye uptake at dye pH ≥ 3.

**Cation Exchange Capacity (CEC)** describes sorbent affinity for sorbate verified by decrease in sorbate concentration in the exchanging solution. CEC reveals the propensity of negative surface charge on an adsorbent exposing its adsorptive potential. In clay surfaces, the negatively charged sites are located in large structural channels and cavities throughout the clay structure. These charges stem from the dissociation of functional surface groups (Si---O---Al, Al---O---H) and correspond to a preferential accumulation of charged species at the interface (Tschapek et al, 1974). Cations in clay can be classified as acidic (H<sup>+</sup> and Al<sup>3+</sup>) or basic (Ca<sup>2+</sup>, K<sup>+</sup>, Mg<sup>2+</sup> and Na<sup>+</sup>) (Grim, in WHO Geneva, 2005).

Even at PZC; the charges from broken edges, exposed OH basal planes (Chi Ma & Eggleton, 1999), amount of Al<sup>3+</sup> that

replaces  $\text{Si}^{4+}$  (Ming & Dixon, 1987) and isomorphous substitution govern clay cation exchange capacity (Grim, in WHO Geneva, 2005).

The low CEC of ACS could imply existence of free negatively charged surface sites typical of cationic dye attraction. The high CEC of the RCS is probable due to crushing broken edges and thermal dehydroxylation which leaves  $\text{Ca}^{+2}/\text{Mg}^{+2}$  vulnerable for cation exchange thus improves MB dye uptake. The CECs of RS and RCS relative to ACS may be pointing that RS and RCS have less free negative surface charges, however may have enough replaceable (exchangeable) cations depending on the pH of the medium.

**Acid activation:** Acid activation of clays limit the possible decomposition of the crystalline structure and increase the specific surface area (Bhattacharyya & Gupta 2009). Higher activation acid concentration is capable of causing adsorbent framework collapse more particularly under severe activation conditions. The activation acid,  $\text{H}_2\text{SO}_4$ , likely has produced a progressive dissolution of the octahedral sheets; the edges of the platelets of the raw clay structure were opened creating micro-porosity between the tetrahedral silicate sheets that maintained the skeleton of the clay mineral and contained the silanol groups thus, both the specific surface area and the pore

diameter increased. Surface area enhancement with modification is reported in Table 1. The high pH of ACS suggests that activation could have altered the acidic structure of the clay making it prone to forming hydrolyzed basic compounds in solution in lieu of the acidic ion,  $\text{SO}_4^{2-}$ .

**Calcination** in clay study has scantily been applied for heavy metal (Aivalioti et al., 2010) mainly on the resolve of its high capacity of improving surface area via porosity enhancement and mineral transformation. Calcination influences the crystalline structure of adsorbent materials hence improves fineness and porosity; surface area. Calcination as applied in this work is based on its propensity of total surface (area) improvement, enhancement of pore volume distribution, clay minerals transformation to suit its use and the enhancement of the reactive properties of the clay minerals. Calcination time and temperature within 4hour and  $750^\circ\text{C}$  respectively have been reported by Aivalioti et al. (2010), Hefne et al. (2008), Talaat et al. (2011), Krishna and Gupta (2006 & 2009). Table 1 illustrates the order of increasing surface areas as  $\text{RS} < \text{RCS} < \text{ACS}$ . The increase can also be attributed to the removal of admixtures or hydroxyls through volatilization at high temperature (Aivalioti et al, 2010).

Table 1: Analytic Characterization

Sample	pH	Acidity		CEC ( $\text{cmolKg}^{-1}$ )	Surface Area ( $\text{m}^2\text{g}^{-1}$ )	Filtration Rate	
		(%)	PZC			Time (Min.)	Rate ( $\text{mL}/\text{m}^2\text{S}$ )
RS	5.52	32	2.67	10.54	22.04	29.00	6.050
RCS	5.41	39	2.46	16.11	30.36	25.00	7.018
ACS	5.72	47	2.50	8.11	40.92	23.63	7.423

**Surface Acidity:** Surface acidity, implying acid strength of the clay surface, defines the proton-donating ability of the clay. Acid strength of clay mineral increases with decreasing amounts of interlayer water. The acidity values as shown in Table 1, affirmed by the exposition of the CEC value indicated the high sorption tendency of the raw and modified clay. Analysis has shown that moderate activation (25–30%) increases the total surface area and the clay acidity (Komadel and Madejová, 2006). The acidity on the report is the amount of the total CEC occupied by the acidic cations ( $\text{H}^{+1}$  and  $\text{Al}^{+3}$ ). The exchangeable acidity, characteristic of CEC revealed 98% of the exchange sites in the soil are occupied by acidic hydrogen and aluminum ions indicating the acidic clay of  $\text{pH} < 5.8$ . The strong acid sites as shown by the acidity values for all samples can be connected with free protons ( $\text{H}^{+}$ ) naturally present and activation-induced.

**Filtration properties (Filtration Rate):** The calculated Filtration rates for the sample are reported in Table 1 which showed that ACS has the highest rate value portraying it is more porous. The low rate for RS could be ascribed organic matter content which was lost on calcination as explained by the increase in the rate of RCS. However, carbonization, a calcination phenomenon is typical of adsorbent pores opening. Considering penetration postulate, filtration rate was acceptable; availing ample time for sorbate-sorbent interaction. The high filtration rates for RCS and ACS

confirmed the porosity and surface area enhancing effect of calcination. While that of the ACS compared to RCS implied the structural changes due to activation. Therefore, the increased rates of RCS and ACS can be aligned to the clay's  $\text{Ca}^{+2}$  and/or  $\text{Al}^{+3}$  content probably formation oxides and encourage sorbent particle aggregation.

**Fourier Transform Infra-Red (FTIR) Spectroscopy:** The FTIR spectra of the clay samples were obtained in the Mid Infrared (MIR) region, a range of  $4000\text{cm}^{-1}$  to  $600\text{cm}^{-1}$ . Mixing and grinding during the sample preparation is known to effect severe changes in the intensities of some absorption bands due to interaction between KBr and the sample. Optical and chemical effects typical of unassigned bands and frequencies can be linked to pressing of KBr-sample into pallet prior to the IR adsorption. The above assertions stand for the unspecified and lost spectra bands of the analyzed samples relative to available standards.

Figure 1 shows the spectra of the respective samples illustrating a marked difference in the spectra of RS and RCS which best depicts that structural changes due to calcination resulted in the disappearance of the spectral band at  $3927.4\text{cm}^{-1}$  characteristic of OH of water. The calcination is typically responsible for dehydroxylation (loss of structural hydroxyl: internal surface OH), possible mineral transformations capable of admixtures formation, and loss of adsorb water.

**Spectra analysis:** The spectra of the samples in Figure 1 above, does not have any close similarity with the compared standard spectra as referred in Vaculikova and Plevova, (2005), spectra data base or literature. This is probably due to sample preparation, presence of multiple admixtures and/or mineral transformation due to thermal treatment. Grounding to powdery form prior to IR analysis has been reported capable of drastic structural and spectral alteration.

In the RS, band at  $3671.22\text{cm}^{-1}$  showing high transmittance and indicating the presence of OH stretching diminished in RCS spectra and disappeared completely in ACS, presumably exposing cation hydroxylation of activation and dehydroxylation due to calcination. The OH-stretching and deformation frequencies were decreased in ACS spectra relative to RCS spectra. The spectra show that:

(i) All the major OH-stretching bands have increased intensities after calcination, with shifts in the frequencies from  $3671.22\text{cm}^{-1}$  in RS to  $3651.78\text{cm}^{-1}$  in RCS and  $3662.19\text{cm}^{-1}$  in ACS.

(ii) RS has SiO-stretching vibrations at  $1084.3$  and  $1222.0\text{cm}^{-1}$  while the calcined samples each (RCS,  $1129\text{cm}^{-1}$  and ACS  $1078.9\text{cm}^{-1}$ ) exhibited one band with a much decreased intensities.

(iii) The intensity of the OH-bending frequency increased in the order  $\text{ACS} > \text{RCS} > \text{RS}$  ( $935.7$ ,  $922.9$  and  $905.10\text{cm}^{-1}$ ) with ACS showing relatively reduced band intensity.

The band frequencies around  $3410\text{-}3920\text{cm}^{-1}$  characteristic of OH of adsorbed water indicated that the clay is a phyllosilicate. Owing to the mixing of various overtones and complexity of clay spectra, various other vibrations have not been assigned. It is worthy to note, vibrations of OH in clay minerals cannot be accurately identified, as water is absorbed by KBr in the OH region (Oinuma & Hayashi, 1965) mainly during sample preparation. Bands beyond  $3800\text{cm}^{-1}$  can be assigned to surface OH from adsorbed water that are not involved in bonding and can very easily be lost on heating. The sharp band at  $3410.5\text{cm}^{-1}$  (characteristic of the zeolitic water of palygorskite) (Madejova & Komadel, 2001; Golden & Dixon, 1990) in RS spectra disappeared upon calcination as the zeolitic water gave way to H-bonded interlayer water that produced spectra bands at  $3425.3$  and  $3478.1\text{cm}^{-1}$  in RCS and ACS. John Coates, (2000) assigned band (sharp doublet) around  $1355\text{-}1360$  (RS,  $1359.6\text{cm}^{-1}$ ) to  $1/2^\circ$  OH in-plane bend.

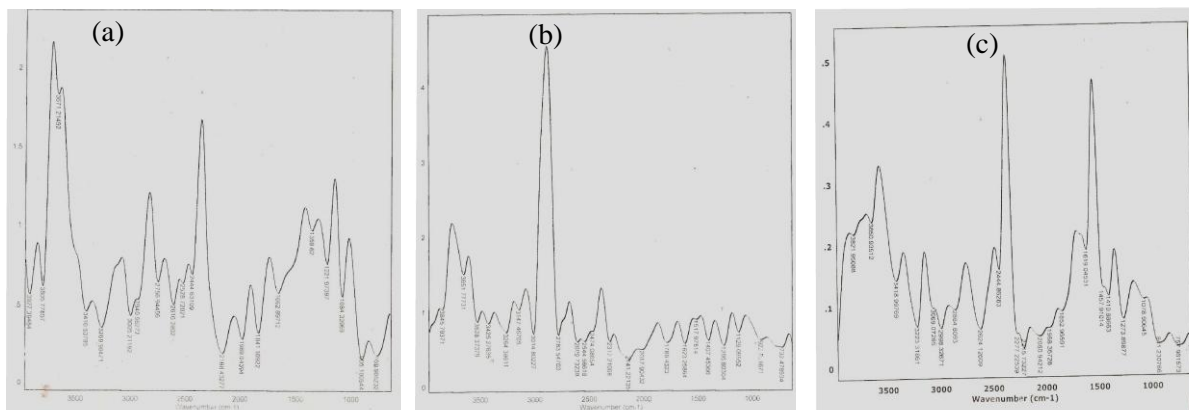


Figure 1: FTIR spectra of (a) RS, (b) RCS and (c) ACS

**Water:** The bands at  $1662.9\text{cm}^{-1}$  and  $1623.3\text{cm}^{-1}$  in RS and RCS indicating OH-scissoring, assigned to *OH-deformation of water*, suggested possible water of hydration in the samples. This agrees with Shoval, et al. (1999): the band around  $1648\text{cm}^{-1}$  corresponds strongly to hydrogen bonded  $\text{H}_2\text{O}$ , whereas the bands around  $1629\text{cm}^{-1}$  are attributed to fairly strong hydrogen bonded  $\text{H}_2\text{O}$  and match the position of the  $\text{H}_2\text{O}$  bending mode of  $\text{H}_2\text{O}_l$ .

The adsorption bands with prominent doublets found around  $3255\text{-}3300\text{cm}^{-1}$  ( $3269.9$ ,  $3264.4$  and  $3297.8\text{cm}^{-1}$ ) conformed to the presence of  $\text{NH}_4$  according to John Coates, (2000). The adsorption bands around  $1402\text{-}1434\text{cm}^{-1}$  can be assigned to  $\text{NH}_4$  deformation of  $\text{NH}_4\text{Br}$  or  $\text{NH}_4$ -clay and the  $\text{CO}_3$  stretching of calcite (Madejova & Komadel, 2001). In agreement with the findings of Saikia et al., (2010), the studied samples exhibit very pronounced and sharp bands around  $1800\text{-}3000\text{cm}^{-1}$  typical of C-H bond stretchings of

organic compounds indicating polyatomic Cn-H-O entities with C bonded to two or three H. Adsorption spectra band found at  $1470\text{-}1475\text{cm}^{-1}$  arises due to  $\text{Na}^+\text{-CO}_3^{2-}$  vibration (McMillan, et al., 1992). The carbonate structure contains isolated  $\text{CO}_3^{2-}$  group with a doubly degenerate symmetric stretch ( $\nu_3$ ) at the region  $1508\text{-}1560\text{cm}^{-1}$  (Parthasarathy et al., 2002). These bands were observed in the studied calcined samples at  $1407.5$  and  $1518\text{cm}^{-1}$  for RCS, and  $1440$  and  $1597.1\text{cm}^{-1}$  for ACS. Observing the spectra of RS, the bands around  $1470\text{-}1475$  and  $1508\text{-}1560\text{cm}^{-1}$  overlapped forming very shallow sloppy shoulders into the band of adsorbed water of deformation. This could imply, the presence of the carbonates characteristic of these bands were overshadowed by the large amount of  $\text{H}_2\text{O}$ . The reduced amount of adsorbed  $\text{H}_2\text{O}$  noticed with the fall in the band frequencies, below  $3850\text{cm}^{-1}$  in the calcined samples gave way for the bands to have sharp doublets indicating the presence of the carbonates.

**B) Adsorption Kinetics Models**

Surface kinetics that tells what happens at the surface, interior/exterior of the adsorbent (adsorption onto surface or desorption into the bulk); Film Diffusion Resistance: exist at the bulk solution/adsorbent surface interface and is controlled by concentration gradient across the interface and limits external surface adsorption; and Pore Diffusion Resistance, a barrier to free flow into adsorbent internal surfaces, characteristic of starving interior surface; explain slow adsorption in liquid/solid system

Describing the dye-clay interaction order, the reaction based kinetic model- Lagergren, Evolich models; and the diffusion based kinetic model- intra-particle diffusion and diffusion resistance models were considered.

**Lagergren Models:** The Lagergren solid capacity equation (1898) was the first rate equation for sorption in liquid/solid system. The first and second order models are often applied together, even when the first seem to fit. This is because, linearity is not a firm criterion for allotting a model to the interactions involved (Bhattacharyya, & Gupta, 2009). The pseudo first order rate is represented as:

$$\frac{dq_t}{dt} = K_1(q_e - q_t) \tag{6}$$

Integrating at  $t = 0; t = t$  and  $q_t = 0; q_t = q_t$  and linearizing gives:

$$\ln(q_{e,exp} - q_t) = \ln(q_{e,cal}) - K_1 t \tag{7}$$

Where  $q_{e,exp}$  is the experimental equilibrium uptake (g/g);  $q_{e,cal}$  is the equilibrium uptake calculated from the intercept;

$q_t$  is experimental uptake at time,  $t$  (g/g);  $K_1$  is the first order rate constant ( $\text{min}^{-1}$ ).

Pseudo second order model predicts the adsorption behavior over a whole time adsorption (Ho, 2006) and the rate mechanism can be expressed as:

$$\frac{dq_t}{dt} = K_2(q_{e,exp} - q_t)^2 \tag{8}$$

At  $t=0; t=t$  and  $q_t = 0; q_t = q_t$ , integration yields

$$\left(\frac{t}{q_t}\right) = \left(\frac{1}{K_2 q_{e,cal}^2}\right) + \left(\frac{1}{q_{e,cal}}\right) t \tag{9}$$

Plot linearity, correlation coefficient, closeness of  $q_{e,exp}$  and  $q_{e,cal}$  and normalized standard deviation  $\Delta q(\%)$  (Ölener, et al. 2008) are considerable criteria to verify and validate the best fit model.

$$\Delta q(\%) = 100 \left( \frac{\sum [(q_{exp} - q_{cal}) / q_{exp}]^2}{(n-1)} \right)^{0.5} \tag{10}$$

The closeness of  $q_{e,exp}$  and  $q_{e,cal}$  as shown in Table 2 revealed that the second order model best describe the kinetic of MB adsorption. The first order did not describe the process probably because: (i)  $K(q_e - q_t)$  did not represent the number of available sites, and (ii)  $\ln(q_e)$  is not equal to the intercept of the plot of  $\ln(q_e - q_t)$  against  $t$ . Therefore, adsorption of MB onto the clay samples is approximated more appropriately by the pseudo-second-order kinetic model.

Table 2: Reaction Based Kinetic Parameters

Sorbent	RS				RCS				ACS			
	C <sub>0</sub> (g/L)	20	25	30	35	20	25	30	35	20	25	30
q <sub>e,exp</sub> (g/g)	2.940	3.365	3.810	4.210	2.509	3.004	3.421	3.857	3.004	3.669	4.055	4.759
<b>Pseudo first order</b>												
q <sub>e,cal</sub> (g/g)	7.071	2.425	3.850	6.141	3.618	4.023	3.792	13.49	1.357	1.744	3.327	5.506
k <sub>1</sub> (min <sup>-1</sup> )	0.076	0.047	0.059	0.079	0.055	0.059	0.058	0.106	0.045	0.049	0.058	0.057
R <sup>2</sup>	0.897	1.000	0.987	0.998	0.958	0.963	0.997	0.971	0.908	0.804	0.997	0.858
Δq(%)	86.85				25.52				45.93			
X <sup>2</sup>	3.385				7.513				4.384			
<b>Pseudo second order</b>												
q <sub>e,cal</sub> (g/g)	3.195	3.546	4.000	4.405	2.762	3.195	3.623	4.049	3.184	3.923	4.255	5.376
k <sub>2</sub> (min <sup>-1</sup> )	0.029	0.039	0.037	0.039	0.026	0.037	0.035	0.038	0.040	0.067	0.037	0.011
H (g/g.min)	0.297	0.493	0.595	0.756	0.200	0.375	0.462	0.625	0.406	1.033	0.673	0.308
R <sup>2</sup>	0.998	0.999	0.999	0.998	0.996	0.998	0.998	0.998	0.998	0.999	0.998	0.993
Δq(%)	7.08				8.20				9.60			
X <sup>2</sup>	0.047				0.055				0.107			
<b>Elovich</b>												
α (g/g.min)	13.036	9.822	7.326	1.627	0.675	3.194	4.417	6.915	3.466	118.1	8.660	1.653
β (g/g)	1.894	2.049	2.262	2.058	2.062	2.262	2.049	1.901	2.283	2.882	1.859	0.923
R <sup>2</sup>	0.778	0.854	0.867	0.995	0.903	0.871	0.854	0.774	0.826	0.712	0.782	0.878

**Evolich Model:** No specific kinetic mechanism can be proposed from the application of the Elovich equation, rather it indicates how strong the sorbates are held on the clay

surface. This model is most often applicable in energetically heterogeneous solid surface and can be expressed as:

$$q_e = (1/\beta)\ln(\alpha\beta) + (1/\beta)\ln t \tag{11}$$

Where  $\alpha$  and  $\beta$  are the Elovich coefficients, representing the initial adsorption rate [(g min<sup>2</sup>)/g] and the desorption coefficient [g/ming] respectively.

**Diffusion based Model:** From a mechanistic point of view for design purpose, the diffusion based kinetics of adsorption predicts the rate-limiting step of the process; exposing the mechanism of adsorbate transfer to and from the adsorbent surface. This transfer is known to occur in steps: film (external) diffusion, pore (intra-particle) diffusion, and sorption on surface sites; however, the overall process may be controlled by one or more steps. In adsorption, the solute transfer is usually characterized by either external mass transfer (boundary layer diffusion) for non-porous media, intra particle diffusion typical of porous matrices, or both combined.

**Intra-particle Diffusion Model** is characterized by the relationship between specific adsorption and the square root of time, given in equation below:

$$q_t = K_i t^{0.5} + I \tag{12}$$

$K_i = K_w/m$  where  $K_w$  is rate of initial intra-particle diffusion (mg/min<sup>1/2</sup>) and  $m$  is mass of adsorbent (g) (Wambu, et al. 2011). The intercept, boundary layer thickness ( $I$ ) elucidates the propensity of diffusion resistance. If the above equation plot presents multi-linearity, it implies two or more steps are involved in the overall adsorption process (Kumar et al., 2010), where the initial inclined portion may be ascribed to film diffusion effect, while the final linear portion may be due to pore diffusion or desorption.

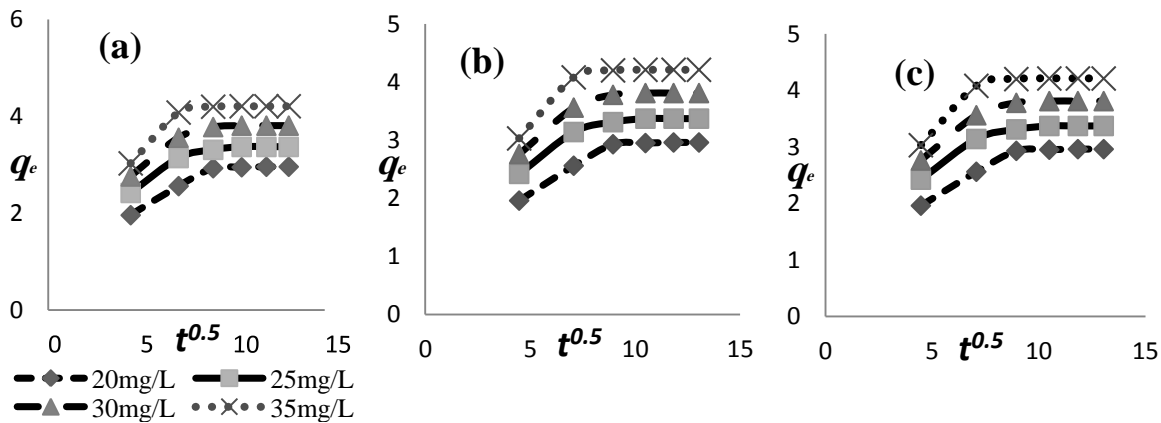


Figure 2: Intra-particle Diffusion plot for (a) RS, (b) RCS, and (c) ACS

The diffusion resistance is ensured by the film thickness around the solid matrix and at the pore entrance. It is controlled by the adsorbate concentration gradient across the film: often, the resistance in spite the film thickness increase as the transfer driving force decreases. Therefore, the measure of the resistance shown by  $I$  and  $M_w$  values depicts the availability of adsorbate in contact with the surface sites. The drop in bulk concentration as adsorption progresses is dependent on the dimensionless quantity  $M_w$  (Wegner Modulus). For  $M_w \leq 0.15$ , the diffusion is resistance free while for  $M_w \geq 4$  implies substantial resistance to diffusion. The effectiveness factor ( $\eta = \frac{C_t}{C_o}$ ) is vital to measure the effect of resistance in the adsorption. It can be presumed in line with Sarici-Ozdemer (2012) that the high concentration gradient/driven force at the process onset is due to high diffusion resistance.

$$M_T = L\sqrt{K/D} \text{ and } M_T^{-2} \equiv D/KL^2 \equiv A/V \tag{13}$$

$$M_w = M_T^2 \eta \quad \text{and } \eta = \frac{M_w A}{V} \tag{14}$$

Where  $C_t$  = concentration around sorbent surface at time ( $t$ ) and  $C_o$  = bulk solution concentration,  $K$  = Adsorption rate constant (m/s),  $D$  = Diffusion coefficient (m<sup>2</sup>/s) and  $L$  = Ratio of surface area to volume of adsorbate solution. *Note:* short pore length ( $L$ ), slow diffusion rate ( $K$ ) or rapid diffusion ( $D$ ) tends to reduce  $M_w$  hence lower the resistance to diffusion.

$$\left(\frac{d(C_t/C_o)}{dt}\right)_{t=0} \Rightarrow \left(\frac{d\eta}{dt}\right) = -K_f \frac{A}{V} = -M_w \frac{A}{V} \tag{15}$$

$$\text{Therefore } \ln \frac{C_t}{C_o} = -M_w A/V t + c \quad (c \approx \text{negligible}) \tag{16}$$

The diffusion of MB onto the clay samples' surfaces as illustrated in the plots of  $q_t$  vs  $t^{0.5}$  and  $\ln C_t/C_o$  vs  $t$ , shown in Fig. 2 and Fig. 3, and reported in Table 3 indicated multi-linearity and significant boundary thickness specifying both mechanisms controlled the MB dye transfer.

From the plot, the early stage is marked by film diffusion which increased with time for about 50mins after which the intra-particle diffusion took over at a steady state dynamic equilibrium. Effectiveness factor ( $\eta$ ) was high, 0.999 at the



initial stage indicating poor adsorption due to predominant diffusion resistance. Beyond 80min,  $\eta$  decreases though significant; indicating neither film-resistance nor intra-particle

diffusion was in total control of adsorbate transfer process. The reverse curve of the resistance model indicates it is an opposing mechanism.

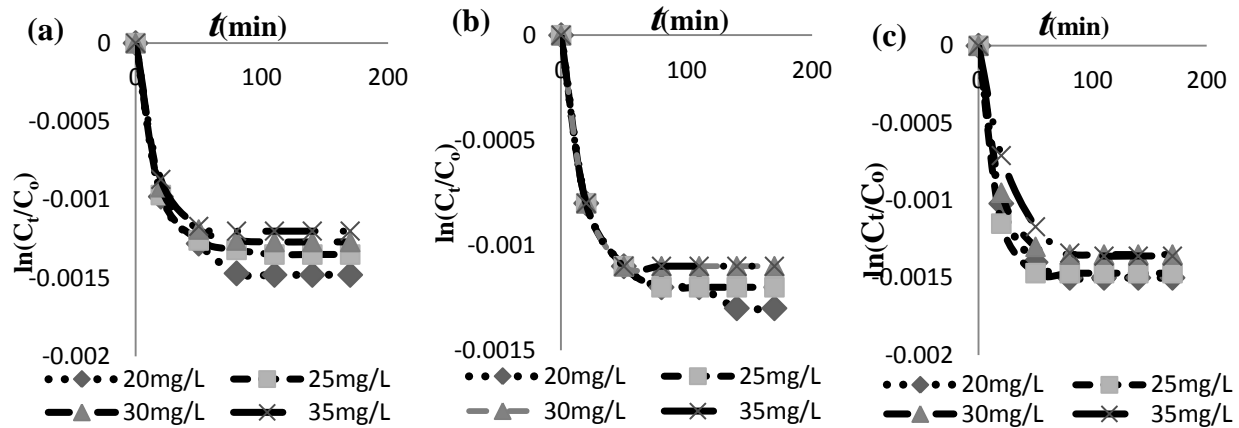


Figure 3: Film Diffusion resistance plot for (a) RS, (b) RCS and (c) ACS

Table 3: Diffusion Based Kinetics Parameters

Sorbent	RS				RCS				ACS			
	C <sub>0</sub> (g/L)	20	25	30	35	20	25	30	35	20	25	30
<b>Intra-particle diffusion</b>												
K <sub>int</sub> (mg/g.min <sup>1/2</sup> )	0.119	0.112	0.102	0.114	0.113	0.101	0.112	0.118	0.100	0.077	0.121	0.251
I	2.541	1.657	2.212	2.877	1.211	1.849	2.152	2.534	1.879	2.811	2.700	1.913
<b>Film diffusion resistance</b>												
M <sub>w</sub> A/V	7E-6	6E-6	5E-6	5E-6	6 E-6	5 E-6	5 E-6	5 E-6	7 E-6	6 E-6	6 E-6	7 E-6
M <sub>w</sub>	5.143	4.408	3.673	3.673	6.072	5.060	5.060	5.060	9.548	8.184	8.184	9.548

**c) Statistical Analysis – Coefficients, Error and Deviation**

The correlation coefficient, R measures the direction of the linear relationship between two variables. R≤1 implies the dependent and independent variables have strong relationship such that as the independent variable increases, the independent variable also increases. R>0.8 is generally described as strong while R<0.5 is weak. Coefficient of Determination, R<sup>2</sup> exposes the degree of variation in variable prediction. It gives the ratio of the explained variable to the total variable. It determines the proportion of experimental data that is on/closest to the line of best fit. An error is required to evaluate the fitness of an isotherm equation to the experimental equilibrium data obtained (Chatterjee, et al. 2009). In this study, Regression coefficients (R<sup>2</sup>) and a nonlinear Chi-square test were performed for all the isotherm models. The Chi-square test statistic can be represented mathematically as:

$$\chi^2 = \sum \left( \frac{(q_e - q_m)^2}{q_m} \right) \quad (37)$$

Where q<sub>m</sub> is the model equilibrium capacity (mg/g) and q<sub>e</sub> is the experimental equilibrium capacity (mg/g). The  $\chi^2$  value is small for q<sub>m</sub> ≈ q<sub>e</sub>, and  $\chi^2$  value increases as q<sub>m</sub> > q<sub>e</sub>.

Thus, it is necessary to analyze the data and confirm the best fit isotherm for this adsorption system using the non-linear Chi-square test. The R, R<sup>2</sup>, X<sup>2</sup> and Δq were determined using the Microsoft’s spreadsheet, Microsoft Excel and shown in Table 2.

The highest R<sup>2</sup> values of the pseudo-second order model (Tab. 3) imply best fit. The table also indicates, besides the observed closeness of q<sub>e,exp</sub> and q<sub>e,cal</sub>, and the highest R<sup>2</sup> which authenticate the linearity and best fit to the kinetic data; the low error (X<sup>2</sup>) which implied the closeness of q<sub>e,exp</sub> and q<sub>e,cal</sub> is realistic and the normalized standard deviation of the Pseudo-second order model which shows a very low deviation of less than 10% for all the samples, confirmed and validated the second order model as the reaction kinetics model for MB uptake onto the clay samples.

**IV. CONCLUSION**

The main purpose of this work is to investigate the inherent characteristics of the clay samples that accounts for its MB adsorption potency and to explore the kinetic mechanism of the uptake. From the results obtained, it follows that Ekowe clay is acidic clay of low PZC. Calcination enhanced the CEC, surface area and filtration capacity of the raw and

activated clay. The FTIR spectra bands revealed that the clay contain inherent admixtures and exposes that chemical and thermal modification is potent the clay transformations. The raw and modified samples showed characteristic adsorption-enhancing PZCs that were below the experimental pH, and the CECs of all the samples were governed by the charges from broken edges, exposed OH basal planes and isomorphous substitution. Generally, the applied modifications enhanced MB dye uptake onto Ekowe clay.

The closeness of  $q_{e,exp}$  and  $q_{e,cal}$  verified by very low statistical error ( $X^2$ ) and normalized standard deviation ( $\Delta q$ ) authenticated that the whole time uptake of MB dye onto the clay samples can be predicted with the Lagergren pseudo second order model. The multi-linear plot of the intra-particle diffusion, the significant boundary layer thickness (I) and the Wegner modulus ( $M_{w \geq 4}$ ) verified that intra-particle diffusion and pore diffusion resistance co-determine the transfer of MB dye to and from the clay adsorption surfaces.

## REFERENCES

- Aivalioti, M., Vamvasakis, I. & Gidaracos, E. (2010). BTEX and MTBE adsorption onto raw and thermally modified diatomite. *Journal of Hazardous Materials*, 178, 136–143.
- Arlette M. C., Ibanez, J. G., & Vasquez-Medrano, R. (2012). Determination of the Point of Zero Charge for Electrocoagulation Precipitates from an Iron Anode. *International Journal of Electrochemical Science*, 7, 6142–6153. Retrieved from <http://www.electrochemsci.org>
- Al-Degs, Y., Khraisheh, M. A. M. & Tutunji, M. F. (2001). Sorption of lead ions on diatomite and manganese oxides modified diatomite. *Water Resources*, 35(15), 3724–3728.
- Appel, C., Ma, Q.L., Rhue, R. D., & Kennelle, E. (2003). Point of zero charge determination in soils and minerals via traditional methods and detection of electroacoustic mobility. *Geoderma*, 113, pp. 77–93.
- ALzaydien, A. S. (2009). Adsorption of Methylene Blue from Aqueous Solution onto a Low-Cost Natural Jordanian Tripoli. *American Journal of Environmental Sciences*, 5(3), 197-208. ISSN 1553-345X
- Ali, S. Z., Athar, M., Salman, M., & Din, M. I. (2011). Simultaneous removal of Pb(II), Cd(II) and Cu(II) from aqueous solutions by adsorption on *Triticum aestivum* – A green approach. *Hydrological Current Resources*, 2, 118. doi:10.4172/2157-7587.1000118
- Abechi, E.S, Gimba, C.E, Uzairu, A., & Kagbu, J.A., (2011). Kinetics of adsorption of methylene blue onto activated carbon prepared from palm kernel shell. *Scholars Research Library Archives of Applied Science Research*, 3(1), 154-164. Retrieved from <http://scholarsresearchlibrary.com/archive.html>
- Bailey, S. E., Olin, T. J., Bricka, R. M., & Adrian, D. D. (1999). A review of potentially low cost sorbents for heavy metals. *Water Resources*, 33, 2469.
- Bhattacharyya, K. G., & Gupta, S. S. (2006). Adsorption of Chromium (VI) from Water by Clays. *Industrial Engineering Chemistry Research*, 45, 7232-7240. DOI: 10.1021/ie060586j CCC.
- Bhattacharyya, K. G., & Gupta, S. S. (2009). Adsorptive Accumulation of Cd(II), Co(II), Cu(II), Pb(II) and Ni(II) ions from water onto Kaolinite: Influence of acid activation. *Adsorption Science & Technology*, 27(1), 47-68.
- Chatterjee, S., Lee, D. S., Lee, M. W., & Woo, S. H. (2009). Enhanced adsorption of Congo red from aqueous solutions by chitosan hydrogel beads impregnated with cetyl trimethyl ammonium bromide. *Bioresource Technology*, 100, 2803 – 2809. doi:10.1016/j.biortech.2008.12.035. Accessible in [www.elsevier.com/locate/biortech](http://www.elsevier.com/locate/biortech)
- Crini, G. (2006). Non-conventional low-cost adsorbents for dye removal: A review. *Bioresource Technology*, 97, 1061–1085.
- Gulnaz, O., Kaya, A., Matyar, F. & Arikan, B. (2004). Sorption of basic dyes from aqueous solution by activated sludge. *Journal of Hazardous Materials*, 108, 183-188.
- Golden, D. C., & Dixon, J. B. (1990). Low-temperature alteration of palygorskite to smectite. *Clays and Clay Minerals*, 38(4), 401-408.
- Ho, Y. S. (2006). Review of second-order models for adsorption systems. *Journal of Hazardous Material*, 136, 681–689.
- Hefne, J. A., Mekhemer, W. K., Alandis, N.M., Aldaye, O.A. & Aljvay, T. (2008). Kinetic and thermodynamic study of the adsorption of Pb (II) from aqueous solution to the natural and treated bentonite. *International Journal of Physical Science*, 3(11), 281-288 <http://mineral.galleries.com/minerals/silicate/clays.htm>
- John Coates, 2000. Interpretation of infrared spectra: A practical approach. In R. A. Meyers (Ed.), *Encyclopedia of Analytical Chemistry* (pp. 10815–10837). Chichester UK: John Wiley & Sons Ltd.
- Komadel, P., Madejova, J., 2006, Chapter 7.1: Acid Activation of Clay Minerals. *Handbook of Clay Science*. Edited by F. Bergaya, B.K.G. Theng and G. Lagaly, *Developments in Clay Science*, 1, 263-287. DOI: 10.1016/S1572-4352(05)01008-1
- Khraisheh, M. A. M., Al-degs, Y. S. & Mcminn, W. A. M. (2004). Remediation of wastewater containing heavy metals using raw and modified diatomite. *Chemical Engineering Journal*, 99, 177 – 184. doi:10.1016/j.cej.2003.11.029
- Kumar, R. P., Varanasi, S & Purushothaman, V. (2010). Investigation of the biosorption mechanisms of Methylene blue onto press mud through kinetic modeling analysis. *Indian Journal of Science and Technology*, 3(1), 44 - 47. ISSN: 0974- 6846
- McMillan, P. F., Wolf, G. H. & Poe, B. T. E. (1992). *Vibrational Properties of Silicate Liquids and Glasses*. *Chemical Geology*, 96 (3-4), 351-356.
- Madejova, J. & Komadel, P. (2001). Baseline studies of the clay minerals society source Clays: Infrared methods. *Clays and Clay Minerals*, 49 (5), 410–432.
- Ma, C. & Eggleton, R. A. (1999). Cation Exchange Capacity of Kaolinite. *Clays and Clay Minerals*, 47(2), 174 - 180.
- Ming, D. W. & Dixon, J. B. (1987). Quantitative Determination of Clinoptilolite in Soils by a Cation-Exchange Capacity Method. *Clays and Clay Minerals*, 35(6), 463 - 468.
- Meier, P. L. & Kahr, G. (1999). Determination of the cation exchange capacity (CEC) of Clay minerals using the complexes of copper(II) ion with Triethylenetetramine and Tetraethylenepentamine. *Clays and Clay Minerals*, 47(3), 386-388.
- Osmanlioglu, A. E., (2007). Natural diatomite process for removal of radioactivity from liquid waste, *Applied Radiation Isotopes*, 65, 17–20.

- Oinuma, K. & Hayashi, H. (1965). IR study of mixed clay minerals. *American Mineral*, 50, 1213-1227.
- Ölenera, M., Tunalib, S., Özcanc, A. S., Özcanc, A. & Gedikbey, T. (2008). Adsorption characteristics of Lead (II) ions onto the clay/poly(methoxyethyl) acrylamide (PMEA) composite from aqueous solutions. *Desalination* 223, 308–322.
- Point\_of\_zero\_charge.n.d. In Wikipedia. Retrieved June 2014; 16:15 from [http://en.wikipedia.org/w/index.php?title=Point\\_of\\_zero\\_charge&oldid=517411264](http://en.wikipedia.org/w/index.php?title=Point_of_zero_charge&oldid=517411264).
- Parthasarathy, G., Chetty, T. R. K. & Haggerty, S. E. (2002). Thermal Stability and Spectroscopic Studies of Zemkorite: A carbonate from the Venkatampalle Kimberlite of Southern India. *American Mineralogist*, 87(10), 1384-1389.
- Rahman M. A., Ruhul A. S. M. & Shafiqul A. A. M. (2012). Removal of Methylene Blue from Waste Water using Activated Carbon prepared from Rice Husk. *Dhaka University Journal of Science*, 60(2), 185-189.
- Shawabkeh, R. A. & Tununji, M. F. (2003). Experimental study and modeling of basic dye sorption by diatomaceous clay. *Applied Clay Science*, 24, 111–120.
- Shoval, S., Yariv, S., Michaelian, K., Lapidés, I., Bou-deuille, M. & Panczer, G. (1999). A fifth OH-stretching band in IR spectra of kaolinites. *Journal of Colloid and Interface Science*, 212(2), 523-529.
- Safa, Y. & Bhatti, H. N. (2011). Adsorptive removal of direct dyes by low cost rice husk: Effect of treatments and modifications. *African Journal of Biotechnology*, 10(16), 3128-3142.
- Saha, P. (2010). Assessment on the Removal of Methylene Blue Dye using Tamarind Fruit Shell as Biosorbent. *Springer Science, Business Media B.V.*, 213, 287–299.
- Sarici-Ozdemir, C. (2012). Adsorption and desorption kinetics behaviour of Methylene Blue onto activated carbon. *Physicochemical Problems of Mineral Processing*, 48(2), 441-454. ISSN 2084-4735. Accessible at [www.minproc.pwr.wroc.pl/journal/](http://www.minproc.pwr.wroc.pl/journal/)
- Saikia, B. J. & Parthasarathy, G. (2010). Fourier Transform Infrared Spectroscopic characterization of kaolinite from Assam and Meghalaya, Northeastern India. *Journal of Modern Physics*, 1, 206-210. doi:10.4236/jmp.2010.14031. Retrieved from <http://www.SciRP.org/journal/jmp>
- Tschapek, M., Tcheichvilit, L., & Wasowski, C. (1974). The Point of Zero Charge (PZC) of Kaolinite and 8io2+a1203 mixtures. *Clay Minerals*, 10, 219 -229.
- Talaat, H. A., El Defrawy, N. M., Abulnour, A. G., Hani, H. A. & Tawfik, A. (2011). Evaluation of Heavy Metals removal using some Egyptian clays. *International Conference of Environmental Science and Technology*, Vol. 6.
- Tóth, J. (2002). *Adsorption: Theory, Modelling, and Analysis*. New York: Marcel Dekker Inc.
- Velmurugan, P., Kumar, R. V. & Dhinakaran, G. (2011). Dye removal from aqueous solution using low cost adsorbent. *International Journal of Environmental Sciences*, 1(7), 1493
- Vaculíková, L. & Plevová, E. (2005). Identification of Clay Minerals and Micas in Sedimentary Rocks. *Acta Geodyn. Geomaterial*, 2[2 (138)], 167-175.
- Wambu E. W., Muthakia, G. K., wa-Thiong'O, K. J. & Shiundu, M. P. (2011). Kinetics and thermodynamics of aqueous Cu(II) adsorption on heat regenerated spent bleaching earth. *Bull Chemical Society Ethiop*, 25(2), 181-190. ISSN 1011-3924.
- World Health Organization, Geneva. (2005). *Environmental Health Criteria 231: Bentonite, Kaolin, and Selected Clay Minerals*. Prepared by Z. Adamis, J. Fodor & R. B. Williams. ISBN 92 4 157231 0 (LC/NLM classification: QV 65)
- Yasin, Y., Hussein, M. Z. & Ahmad, F. H. (2007). Adsorption of Methylene Blue onto treated activated carbon. *The Malaysian Journal of Analytical Sciences*, 11(11), 400 - 406.